SLAC–PUB–7543
March, 1998

TESTING UNRUH RADIATION WITH ULTRA-INTENSE LASERS*

PISIN CHEN
Stanford Linear Accelerator Center
Stanford University, Stanford, CA 94309
and

TOSHI TAJIMA
Department of Physics
University of Texas, Austin, TX 78712

ABSTRACT

We point out that using the state-of-the-art (or soon-to-be) intense ultrafast laser technology, violent acceleration that may be suitable for testing general relativistic effects can be realized through the interaction of a high intensity laser with a plasma. In particular, we demonstrate that the Unruh radiation is detectable, in principle, beyond the conventional radiation (most notably the Larmor radiation) background noise, by taking advantage of its specific dependence on the laser power and distinct character in spectral-angular distributions.

Submitted to *Physical Review Letters.*

* Work supported by Department of Energy contract DE–AC03–76SF00515.

General relativity (GR) is by birth a classical theory. The celebrated discovery by Hawking[1] of the black hole radiation links the GR to quantum mechanics and thermodynamics in one stroke. While the ultimate theoretical understanding of the Hawking radiation, for example through the superstring theory[2], is still in progress, the fundamental importance of the Hawking radiation is hardly questionable. Subsequent to Hawking's discovery, Unruh[3] established that similar radiation can also occur for a "particle detector" under acceleration. Without resorting to detail arguements, one can readily appreciate such a notion intuitively based on the equivalence principle. While the celestial observations of GR effects are clearly important, one wonders if by means of extremely violent acceleration in the laboratory setting these effects can be detected or tested by controlled experiments.

There have been proposals for laboratory detection of the Unruh effect[4]. For example, Yablonovich[5] proposed to detect the Unruh radiation using ionization fronts in solids. Darbinyan et at.[6] proposed to test it through the crystal channeling phenomena. Since the sought-after effects are typically extremely weak , the most severe problem would be the struggle against paramount background signals. Thus the challenge in general is to find a physical setting which can maximally enhance the signal above its competing backgrounds.

It is known that plasma wakefields excited by either a laser pulse[7] or an intense electron beam[8] can in principle provide an acceleration gradient as high as100 GeV/cm, or $10^{23} g_{\oplus}$. Such acceleration relies on the collective perturbations of the plasma density excited by the driving pulse and restored by the immobile ions, and therefore is an effect arisen over a plasma period. There is in fact another aspect of laser-plasma interaction. Namely, when a laser is ultra-relativistic (i.e., $a_0 \equiv eE_0/mc\omega_0 \gg 1$), the plasma electrons under the direct influence of the laser

can be instantly "snowplowed" forward in every laser cycle (which is typically much higher frequency than that of the plasma), resulting in a intermittant acceleration that is much more violent than that provided by the plasma wakefields. For the Petawatt-class lasers currently under development[9], 10 TeV/cm, or $10^{25} g_{\oplus}$, will be possible for these "snowplow" accelerations in the near future.

Although the classical equivalent of the acceleration exerted on a nucleon bound to a nucleus can be as large as $a_{\rm nuclear} \sim 10^{28} g_{\oplus}$, it is well-known from quantum mechanics that the notion of classical trajectory and acceleration is not justified in subatomic systems. By the same token one should not expect any GR effect to be generated during high energy particle collisions where, if the notion of classical particle motion was wrongly applied, the hard scattering during a very brief moment would suggest an extremely violent acceleration. Furthermore, as will be addressed in more details below, even if the notion of classical acceleration is valid in a physical system, there is also the question of uniformity and duration of such accelerations for the Unruh effect to be applicable. The outstanding character of our system is that the snowplow acceleration is macroscopic and can be well described by classical electrodynamics, and therefore the Unruh effect associated with violent acceleration can be readily applied.

According to Davies[10] and Unruh[3], a uniformly accelerated particle finds itself imbeded in a thermal heat bath with temperature

$$kT = \frac{\hbar \alpha}{2\pi c} \quad , \tag{1}$$

where α is the constant proper acceleration of the particle. In the standard treatment, an internal degree of freedom of the accelerated particle is invoked as a means to detect the Unruh effect. This can be, for example, a monopole moment (interacting with

a scalar field)[11,12], or the spin of an electron (interacting with EM fields)[13]. Since the agency that we rely on for the violent acccleration is electromagnetic and acts only on charged particles, we consider an electron, the lightest charged particle, as our particle detector. As was shown by Bell and Leinaas[12], the manifestation of the Unruh effect through the equilibrium degree of spin polarization would require an unphysically long time in the case of a linear acceleration, yet for such an effect in a circular motion the Thomas precession complicates the issue. In our approach, we do not invoke any internal degree of freedom. Rather, we rely on the quivering motion of the electron under the influence of the nontrivial vacuum fluctuations, and look for the emitted photons so induced as our signals.

To be sure, the Unruh radiation is not a "new" radiation. Using the standard field theory (in this case quantum electrodynamics), one should in principle be able to arrive at the same result when properly taking particle radiation reaction into account. Treating the problem in the instantaneous proper frame and invoking the particle response to the thermal vacuum fluctuations, however, help to elucidate the phenomenon through a very intuitive picture in the spirit of the fluctuation-dissipation theorem[14] in thermodynamics.

We assume that in the leading order the accelerated electron is "classical", with well-defined acceleration, velocity and position. Therefore we can introduce a Rindler transformation[15] so that the electron is described in its instantaneous proper frame. Also at this level the linearly accelerated electron will execute a classical Larmor radiation. As a response to the Larmor radiation, the electron reacts to the vacuum fluctuations with a quivering motion in its proper frame. This in turn triggers additional radiation. We assume that this quivering motion is nonrelativistic in the

proper frame, and the interaction Hamiltonian can be written as

$$\mathcal{H}_I = -\frac{e}{mc}\vec{p}\cdot\vec{A} = -e\vec{x}\cdot\vec{E} \quad . \tag{2}$$

The probability of the emission of a photon with energy $\omega = \mathcal{E}' - \mathcal{E}$ is

$$\begin{aligned} N(\omega) =& \frac{1}{\hbar^2}\int d\sigma \int d\tau |\langle 1_{\vec{k}}, \mathcal{E}'|\mathcal{H}_I|\mathcal{E}, 0\rangle|^2 \\ =& \frac{e^2}{\hbar^2}\sum_{i,j}^{3}\int d\sigma \int d\tau e^{-i\omega\tau}\langle x_i(\sigma)x_j(\sigma)\rangle\langle E_i(\sigma-\tau/2)E_j(\sigma+\tau/2)\rangle \quad , \end{aligned} \tag{3}$$

where σ and τ are the absolute and relative proper time, respectively. The τ dependence of the position operator has been extracted to the phase due to a unitary transformation. The last bracket is the well-known autocorrelation function for the fluctuations of the electric field in the Rindler vacuum,[16] i.e.,

$$\langle E_i(\sigma-\tau/2)E_j(\sigma+\tau/2)\rangle = \delta_{ij}\frac{4\hbar}{\pi c^3}\left(\frac{\alpha}{2c}\right)^4 \sinh^{-4}\left(\frac{\alpha\tau}{2c}\right) \quad , \qquad i,j = 1,2,3. \tag{4}$$

With a change of variable $s = \alpha\tau/2c$, we find

$$\frac{dN}{d\sigma} = \frac{1}{2\pi}\frac{e^2}{\hbar c^3}\left(\frac{\alpha}{c}\right)^3\langle x^2\rangle \int_{-\infty}^{+\infty} ds \exp\left(-is\frac{2c\omega}{\alpha}\right)\sinh^{-4}(s-i\epsilon) \quad , \tag{5}$$

where $\langle x^2\rangle = \sum_i^3\langle x_i^2\rangle$. This integral has poles at $s = n\pi i$, and is periodic every $\Delta s = \pi i$. Thus it can be easily performed by returning the contour along the line $\mathrm{Im}s = \pi$, and we get

$$\frac{dN}{d\sigma} = \frac{e^2}{3\hbar c^3}\left(\frac{\alpha}{c}\right)^2\langle x^2\rangle\left[2\omega + \left(\frac{c}{\alpha}\right)^2\omega^3\right]\left(e^{2\pi c\omega/\alpha}-1\right)^{-1} \quad . \tag{6}$$

The expectation value of x^2 fluctuates due to the random absorption of quanta from the vacuum fluctuations. From the uncertainty principle we have $\langle x_i^2\rangle\langle p_i^2\rangle \gtrsim \hbar^2$.

By absorbing a quanta of frequency ω, the corresponding change of momentum is $\langle p_i^2 \rangle = \langle p^2 \rangle / 3 = (2/3) m\hbar\omega$. We shall thus assume that

$$\langle x^2 \rangle = \sum_i^3 \langle x_i^2 \rangle \sim \frac{9}{2} \frac{\hbar}{m\omega} \quad . \tag{7}$$

Note that this expression is invalid when the quivering motion becomes relativistic, i.e., $\langle p^2 \rangle \gtrsim (mc)^2$. Beyond this limit a fully relativistic treatment is necessary, and higher order processes such as e^+e^- pair production should be included. Taking the typical frequency of the vacuum fluctuation spectrum, $\omega \sim kT/\hbar$, the nonrelativistic approximation corresponds to the constraint that $kT \lesssim mc^2$. Correspondingly, this means the fluctuations of the electron position in our case is larger than the Compton wavelength, i.e., $\langle x^2 \rangle \gtrsim \lambda_c{}^2$, which is consistent with our semi-classical treatment. This range of validity of our approximation is physically unrelated to the well-known issue of *Zitterbewegung* for an inertial electron[17]. But it is interesting to recall that an unaccelerated electron also jiggles under the zero-point fluctuations of the Minkowski vacuum, yet with $\langle x^2 \rangle \lesssim \lambda_c{}^2$ at a frequency $2c/\lambda_c$. This, as we know, will never constitute any radiation.

To find the radiation power, one should insert Eq(7) and further integrate Eq.(6) over $\hbar d\omega$, which diverges in the infrared limit. In reality, however, the duration of acceleration, τ_a, is always finite, which sets a cutoff frequency at $\omega_a \sim 1/\tau_a$. Therefore we introduce a regularization through an infrared cutoff, ω_a, and find

$$\frac{dI_v}{d\sigma} \approx \int_{\omega_a}^{\infty} \hbar d\omega \frac{dN}{d\sigma} \approx \frac{3}{4\pi} \frac{r_e \hbar}{c} \left(\frac{\alpha}{c}\right)^3 \times \begin{cases} (c/\alpha\tau_a)^2 \exp(-2\pi c/\alpha\tau_a), & \tau_a \ll 2\pi c/\alpha, \\ 2\log(\alpha\tau_a/2\pi c) \quad , & \tau_a \gtrsim 2\pi c/\alpha. \end{cases} \tag{8}$$

We see that if the time for acceleration is less than the characteristic time $\tau_c \equiv 2\pi c/\alpha$, then this radiation is exponentially suppressed.

For the sake of simplicity, we treat the laser as a plane EM wave. Let the laser be linearly polarized in x-direction and propagate in the z-direction, with amplitude $E = E_0 \cos k_0\zeta$, where $\zeta = z - v_{ph}t$ is the coordinate of the comoving frame. The normalized vector potential is then $A(\zeta) = [eE_0/mc\omega_0] \sin k_0\zeta \equiv a_0 \sin k_0\zeta$, where a_0 is the conventional dimensionless laser strength parameter. The state-of-the-art, or soon-to-be, laser technology can provide an intensity so high that $a_0 \gtrsim 100$ is attainable.[9] In our conception, the accelerated electrons are provided by a low temperature plasma. This, in principle, induces a collective reaction from the plasma to the laser through the modification of the index of refraction, $n = \sqrt{1 - (\omega_p/\omega_0)^2} \lesssim 1$, where $\omega_p = c\sqrt{4\pi r_e n_p}$ is the plasma frequency.

The Lorentz force equations for a plasma electron driven by a linearly polarized laser , where its magnetic field is related to the electric field by $B_y = nE_x \equiv nE$, can be written as

$$\begin{aligned} \frac{dp_x}{dt} &= -en\beta_z E \quad , \\ \frac{dp_z}{dt} &= -e(1 - n\beta_x)E \quad . \end{aligned} \tag{9}$$

For a plasma electron initially at rest, its subsequent velocity and energy as a function of ζ in the lab frame can be solved exactly from the above equations. In the regime of our interest it can be shown, with the approximation $\sqrt{[1 + A(\zeta)^2](1 - n^2) + 1} \simeq 1$, that

$$\begin{aligned} \beta_x(\zeta) = \frac{A(\zeta)}{\gamma} \quad ; \qquad \beta_z(\zeta) &= \frac{n}{1+n^2}\frac{A(\zeta)^2}{\gamma} \quad ; \\ \gamma(\zeta) &= \frac{1 + n^2 + A(\zeta)^2}{1 + n^2} \quad . \end{aligned} \tag{10}$$

Note that, as $A(\zeta)$ is periodic, the electron returns to a full stop every half-cycle, where $A(\zeta) = 0$. Taking time derivatives on β_x and β_z, and making Lorentz transformation to the proper frame, it can be shown that the magnitude of the proper acceleration

is simply

$$\alpha = ca_0\sqrt{\omega_0^2+\omega_p^2}\cos k_0\zeta \approx ca_0\omega_0\cos k_0\zeta \quad . \tag{11}$$

Thus in the limit $\omega_p \ll \omega_0$, the plasma effect on the proper acceleration is negligible. It is clear that the maximum acceleration occurs at every half laser cycle, with phases $\eta = k_0\zeta = 0, \pi, 2\pi, ...$, which coincide with the phases where the electron comes to rest.

As can be seen from Eq.(10), since $\beta_x \propto A$ while $\beta_z \propto A^2$, the electron is initially accelerated from rest in the transverse direction. But for the case where $a_0 \gg 1$, the motion is rapidly bent towards the direction of laser propagation (in z). This helps the electron to remain in phase with the laser oscillation for a much longer time compared with the nonrelativistic case. There still is, nevertheless, a slight amount of "phase slippage" incured to the electron versus the laser phase. The phase advance of the electron is

$$\frac{d\eta}{dt} = k_0(v_z - v_{ph}) = \frac{\omega_0}{n}\left(\beta_z - \frac{1}{n}\right) \quad . \tag{12}$$

As we discussed earlier, to avoid exponential suppression we look for a minimum acceleration time $\tau_a \gtrsim \tau_c = 2\pi c/\alpha$. The corresponding characteristic laboratory time t_c for acceleration, through Rindler transformation, is then

$$t_c = \frac{c}{\alpha}\sinh(\tau_c\alpha/c) = \frac{c}{\alpha}\sinh(2\pi) \quad . \tag{13}$$

Integrating Eq.(12) from 0 to $\pm t_c/2$, and assuming that the resultant phase slippage $\eta_c \ll 1$ while $a_0\eta_c \gg 1$, we find the phase slippage to be

$$\pm\eta_c = \pm\frac{1}{a_0}(3\sinh 2\pi)^{1/3} \quad . \tag{14}$$

Thus to ensure the uniformity of acceleration during a time t_c, it is necessary that

$\cos\eta_c \approx 1-(\eta_c)^2/2 \approx 1$, or $a_0 \gg (3\sinh 2\pi)^{1/3}/\sqrt{2} \sim 6.6$. As we will discuss below, we assume an ultra-intense laser where $a_0 \sim 100$, thus the nonuniformity of the proper acceleration during this characteristic time is less than 0.5%, and we shall from here on simply assume $\alpha = ca_0\omega_0$ within the time τ_c.

At the classical level, the same linear acceleration induces a Larmor radiation. The total Larmor radiation power is

$$\frac{dI_{_L}}{dt} = \frac{2}{3}\frac{e^2}{m^2c^3}\left(\frac{dp_\mu}{d\tau}\frac{dp^\mu}{d\tau}\right) = \frac{2}{3}\frac{r_e m\alpha^2}{c} \quad , \tag{15}$$

where Eqs. (10) and (11), and the identity $d\gamma\beta_z/d\tau = d\gamma/d\tau$, which is a direct consequence of the Lorentz force equations, have been invoked. This means that the contribution to the relativistic Larmor radiation is predominantly from the trasverse acceleration by the laser electric field. As the radiation power is a Lorentz invariant quantity, the relative yield between the Unruh radiation (Eq.(8)) and the Larmor radiation in each half-cycle is

$$\frac{dI_{_U}/dt}{dI_{_L}/dt} \approx \frac{9}{4\pi}\frac{\lambda\!\!\!^{-}_c\alpha}{c^2}\log(\alpha\tau_a/2\pi c) \quad . \tag{16}$$

In our particular setting the phase-slippage increases rapidly due to the hyperbolic dependence of t_c on τ_c and the proper acceleration decreases accordingly. It is therefore adequate to assume that $\tau_a \gtrsim \tau_c = 2\pi c/\alpha$ and $\log(\alpha\tau_a/2\pi c) \sim \mathcal{O}(1)$ in our case. Consider the Petawatt laser currently under development [9], where $\omega_0 \sim 2\times 10^{15}\mathrm{sec}^{-1}$ and $a_0 \sim 100$. This gives $(dI_{_U}/dt)/(dI_{_L}/dt) \sim 3\times 10^{-4}$. To have the Unruh radiation power breaking even with that of Lamor radiation, one would need a laser power ($\propto a_0^2$) more than 7 orders of magnitude larger, or an acceleration as large as $\sim 3\times 10^{31}\mathrm{cm/sec}^2 \sim 3\times 10^{28} g_\oplus$, which is beyond the reach of current laser technology. However, the time structure of these radiations and their different characters in

spectral-angular distributions and polarizations help to much relax the demand on acceleration for detectability.

We have shown that the relative phase advance of the electron for emitting typical Unruh photons is a small fraction of the laser half-cycle (cf. Eq.(14)), and have a much sharper temperal profile than that for the Larmor radiation. Because of the snowplow mechanism, the electron rapidly becomes relativistic and is bent forward. As a result the time laps for every period of motion is much longer than the laser period. Roughly, the time separation between successive Unruh signals (for each π-phase slippage) scales as a_0^2:

$$\Delta t \sim \gamma\pi/\omega_0 = (1 + a_0^2/2)\pi/\omega_0 \gg 1/\omega_0 \gg t_c \quad . \tag{17}$$

Therefore it should be possible to set up temporal gates where signals from different periods can be isolated if a thin "film" of plasma is irradiated.

In our treatment the thermal fluctuation is isotropic (cf. Eq.(4))[18] in the electron's proper frame. The radiation induced is therefore also isotropic. Since at each half-cycle by the time when the electron has been accelerated for a time $t_c/2$ from rest, its energy would be $\gamma_c \approx 1 + A^2(\eta_c)/2 \approx 1 + (3\sinh 2\pi)^{2/3}/2 \gg 1$, the Unruh radiation is highly forward boosted in the lab frame. Inserting the proper acceleration $\alpha = ca_0\omega_0$ into Eq.(8), and transforming back to the lab frame with small-angle expansion, the angular distribution becomes

$$\frac{dI_U}{dtd\Omega} \simeq \frac{1}{2\pi^2}\frac{r_e\hbar}{c}\frac{\omega_0^3 a_0^3}{(1+\gamma_c^2\theta^2)^3} \quad . \tag{18}$$

As the Larmor radiation is essentially induced by the transverse acceleration, it

is polarized and its angular distribution in the small (θ, ϕ) polar angle expansion is[19]

$$\frac{d^2 I_{_L}}{dtd\Omega} \simeq \frac{2r_c mca_0^2\omega_0^2}{(1+\gamma_c^2\theta^2)^3}\Big[1 - \frac{4\gamma_c^2\theta^2(1-\phi^2)}{(1+\gamma_c^2\theta^2)^2}\Big] \quad . \tag{19}$$

It is clear that the radiation power is minimum at $(\theta, \phi) = (1/\gamma_c, 0)$, where $d^2 I_{_L}/dtd\Omega = 0$. Consider a detector which covers an azimuthal angle $\Delta\phi = 10^{-3}$ around this "blind spot", and an opening polar angle, $\Delta\theta \ll 1/\gamma_c$. Then the partial radiation power for the Unruh signal would dominate over that for the Larmor within this solid angle.

To be sure, there are other types of radiation backgrounds in addition to the Larmor radiation. The snowplowed plasma electrons will interact with the plasma ions and trigger the conventional bremsstrahlung. The cross section of bremsstrahlung for an unscreened hydrogen nucleus per unit photon energy is well-known: $d\chi/d\hbar\omega \sim (16/3)\alpha r_e^2 \ell n(EE'/mc^2\omega)$. Assuming a frequency window of $\Delta\omega/\omega_u \sim 0.1$ and a temporal gate of $\Delta t \sim 2 \times 10^{-15}$sec, we find that, for the laser parameters discussed above, the plasma density has to be lower than $n_p \lesssim 10^{18}/\text{cm}^3$ in order that the bremsstrahlung signals be less than that from the Unruh effect, which is not a severe restriction.

We have demonstrated that the Unruh radiation can in principle be detectable against the backgrounds from the conventional radiations using the frontier laser technology and the various experimental techniques. The violent, macroscopic acceleration provided by the snowplow mechanism available from ultra-relativistic lasers can also be a useful tool to test other salient features of general relativity in the laboratory setting. This should open up a brand new window to peek into foundations of physics.

REFERENCES

[1] S. W. Hawking, *Nature* **248** (1974) 30; S. W. Hawking, *Commun. Math. Phys.* **43** (1975) 199.

[2] A. Strominger and C. Vafa, *Phys. Lett.* **B379** (1996) 99.

[3] W. Unruh, *Phys. Rev. D* **14** (1976) 870.

[4] For a review, see, for example, H. C. Rosu, *Int. J. Mod. Phys. D* **3** (1994) 545.

[5] E. Yablonovich, *Phys. Rev. Lett.* **62** (1989) 1742.

[6] S. M. Darbinyan, K. A. Ispiryan, M. K. Ispiryan, and A. T. Margaryan, *JETP Lett.* **51** (1990) 110.

[7] T. Tajima and J. M. Dawson, *Phys. Rev. Lett.* **43** (1979) 267.

[8] P. Chen, J. M. Dawson, R. Huff, and T. Katsouleas, *Phys. Rev. Lett.* **54** (1985) 693.

[9] M. Perry and G. Mourou, *Science* **264** (1994) 917.

[10] P. C. W. Davies, *J. Phys. A* **8** (1975) 609.

[11] B. S. DeWitt, in *General Relativity*, eds. S. W. Hawking and W. Israel (Cambridge University Press), 1979.

[12] N. D. Birrell and P. C. W. Davies, *Quantum Fields in Curved Space*, (Cambridge University Press), 1982.

[13] J. S. Bell and J. M. Leinaas, *Nulc. Phys.* **B212** (1983) 131.

[14] R. Kubo, *J. Phys. Soc. Japan* **12** (1957) 570.

[15] W. Rindler, *Essential Relativity*, (New York: Van Norstrand), 1969.

[16] T. H. Boyer, *Phys. Rev. D* **21** (1980) 2137.

[17] J. D. Bjorken and S. D. Drell, *Relativistic Quantum Mechanics*, (McGrow-Hill), 1964.

[18] It has been argued that the vacuum fluctuations in this case is not entirely isotropic. see for example, K. Hinton, P. C. W. Davies, and J. Pfautsch, *Phys. Lett.* **120B** (1983) 88. But we shall ignore it in our discussion.

[19] J. D. Jackson, *Classical Electrodynamics*, second ed. (John Wiley & Sons), 1975.

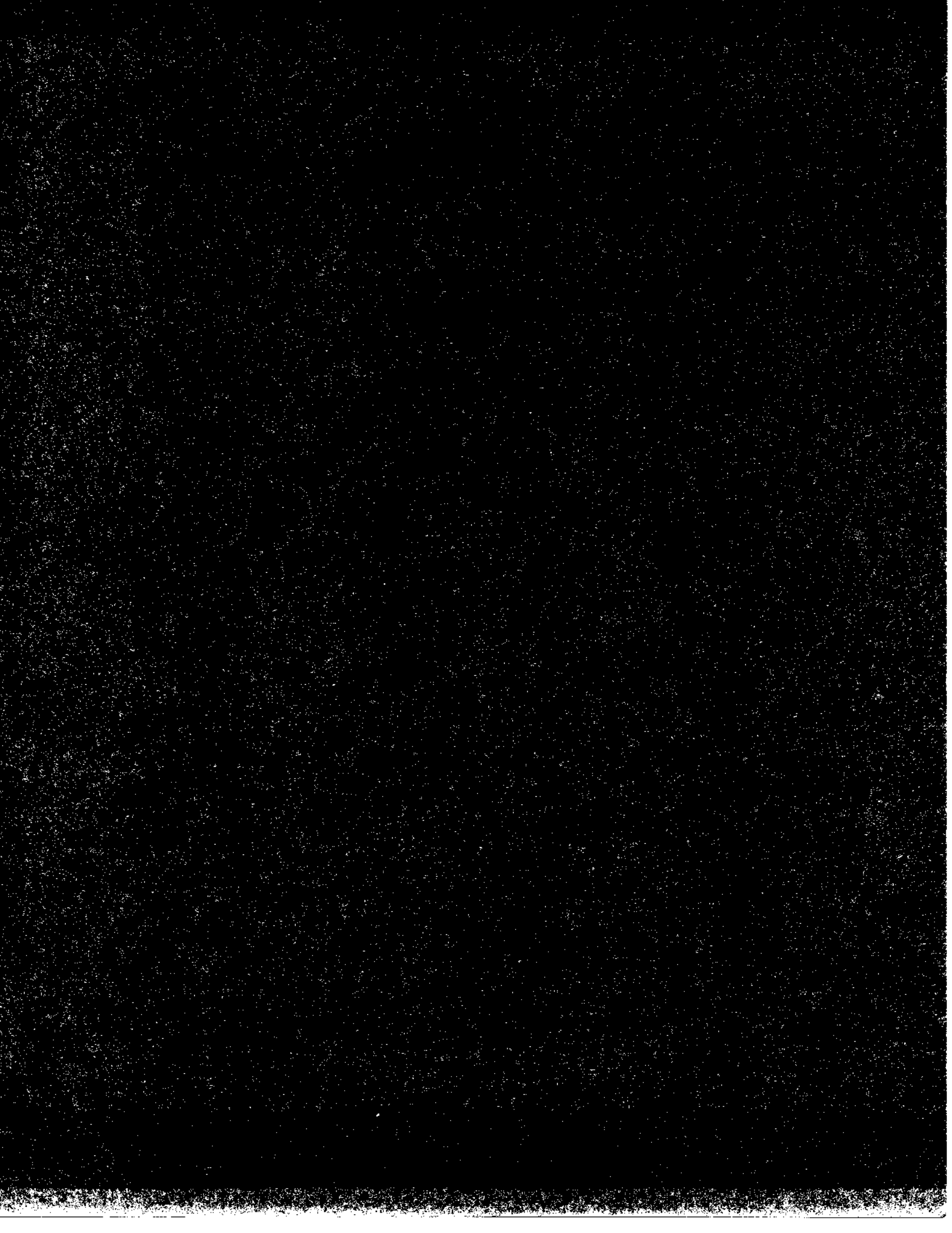

DE-FG03-96ER-54346-790 IFSR #790

Studies of Laser-Driven 5 TeV e^+e^- Colliders in Strong Quantum Beamstrahlung Regime

M. XIE,[1] T. TAJIMA, K. YOKOYA,[2] AND S. CHATTOPADHYAY[1]
Institute for Fusion Studies
The University of Texas at Austin
Austin, Texas 78712 USA

[1]Lawrence Berkeley National Laboratory
[2] Koh-Enerugi Kenkyusho, High Energy Lab., Japan

June 1997

Studies of Laser-Driven 5 TeV e^+e^- Colliders in Strong Quantum Beamstrahlung Regime

M. Xie[1], T. Tajima[2], K. Yokoya[3]
and S. Chattopadhyay[1]

[1] *Laurence Berkeley National Laboratory, USA*
[2] *University of Texas at Austin, USA*
[3] *KEK, Japan*

Abstract.
We explore the multidimensional space of beam parameters, looking for preferred regions of operation for a e^+e^- linear collider at 5 TeV center of mass energy. Due to several major constraints such a collider is pushed into certain regime of high beamstrahlung parameter, Υ, where beamstrahlung can be suppressed by quantum effect. The collider performance at high Υ regime is examined with IP simulations using the code CAIN. Given the required beam parameters we then discuss the feasibility of laser-driven accelerations. In particular, we will discuss the capabilities of laser wakefield acceleration and comment on the difficulties and uncertainties associated with the approach. It is hoped that such an exercise will offer valuable guidelines for and insights into the current development of advanced accelerator technologies oriented towards future collider applications.

INTRODUCTION

It is believed that a linear collider at around 1 TeV center of mass energy can be built more or less with existing technologies. But it is practically impossible to go much beyond that energy without employing a new, yet largely unknown method of acceleration. However, apart from knowing the details of the future technologies, certain collider constraints on electron and positron beam parameters are considered to be quite general and have to be satisfied, e.g. available wall plug power and the constraints imposed by collision processes: beamstrahlung, disruption, backgrounds, etc. Therefore it is appropriate to explore and chart out the preferred region in parameter space based on these constraints, and with that hopefully to offer valuable guide-

lines for and insights into the current development of advanced accelerator technologies oriented towards future collider applications.

Taking such a point of view, we examine collider performance at the final interaction point (IP) of a e^+e^- collider over a large space of beam parameters. We show that it becomes increasingly necessary at higher energy to operate colliders in high Υ regime and use to our advantage the quantum effect to suppress beamstrahlung. Although the quantum suppression effect was known and studied before with simple models [1–4], it has not been checked with full-blown simulation at high Υ regime that we are considering in this paper. As will be shown later, there are indeed several surprising features revealed by our simulations, in particular in the differential luminosity spectrum, which is a crucial factor for colliders.

Given beam parameters that are confirmed by simulation to be within acceptable level of beamstrahlung, we then discuss its implications for laser-driven acceleration. In particular we examine general characteristics and capabilities of laser wakefield acceleration and comment on the difficulties and uncertainties associated with the approach.

COLLIDER CONSIDERATIONS

In this section we will first discuss major collider requirements and constraints and organize the beam parameters in a way more convenient for exploration. We then scan the parameter space to find optimal regime of operation, and discuss its characteristics, as well as design options and trade-offs. These optimal designs are shown to be in high Υ regime. The collider performance at high Υ regime is examined with CAIN [5] simulations.

IP Requirements

The primary drive for developing ever more advanced accelerators is to expand both energy and luminosity frontiers for high energy physics applications. An important collider performance parameter is the geometrical luminosity given by $\mathcal{L}_g = f_c N^2/4\pi\sigma_x\sigma_y$ where f_c is the collision frequency, N is the number of particles per bunch, σ_x and σ_y are, respectively, the horizontal and vertical rms beam sizes at the IP. The real luminosity, however, depends on various dynamic processes at collision. Among them the most important ones are beamstrahlung and disruption [6]. These two processes are characterized by the beamstrahlung parameter $\Upsilon = 5r_e^2\gamma N/6\alpha\sigma_z(\sigma_x + \sigma_y)$, and the disruption parameter $D_y = 2r_e N\sigma_z/\gamma\sigma_y(\sigma_x + \sigma_y)$, where γ is the Lorentz factor, r_e the classical electron radius, α the fine structure constant, and σ_z the rms bunch length. Beamstrahlung is in classical regime if $\Upsilon \ll 1$, and strong quantum regime if $\Upsilon \gg 1$. The physical effect of beamstrahlung is not directly reflected in the magnitude of Υ, but rather it is

more conveniently monitored through the average number of emitted photons per electron $n_\gamma = 2.54\,(\alpha\sigma_z\Upsilon/\lambda_c\gamma)\,U_0(\Upsilon)$ and relative electron energy loss $\delta_E = 1.24\,(\alpha\sigma_z\Upsilon/\lambda_c\gamma)\,\Upsilon U_1(\Upsilon)$. where $\lambda_c = \hbar/mc$ is the Compton wavelength, $U_0(\Upsilon) \approx 1/(1+\Upsilon^{2/3})^{1/2}$, and $U_1(\Upsilon) \approx 1/(1+(1.5\Upsilon)^{2/3})^2$.

So far we have given the major constraints imposed at the collision, which require n_γ and δ_E not be too large to cause luminosity degradation. Generally speaking, when these requirements are satisfied, other deteriorating effects such as pair creation and hardronic background will also be small [6]. Another major constraint for collider design is the available wall plug power which limits the beam power, given accelerator efficiency. We define the average power of both colliding beams $P_b = 2E_bNf_c$, the center of mass energy $E_{cm} = 2E_b$, and the beam energy $E_b = \gamma mc^2$.

It is noted from all the formulas given above that there are only six independent parameters and they are chosen for convenience to be $\{E_{cm},\ \mathcal{L}_g,\ P_b,\ R,\ N,\ \sigma_z\}$, where R is the aspect ratio σ_x/σ_y. For collider design considerations we are interested in monitoring six quantities $\{f_c, \sigma_y, \Upsilon, D_y, n_\gamma, \delta_E\}$, and they are expressed in terms of the six independent parameters as follows

$$f_c = \left(\frac{P_b}{E_{cm}}\right)\left(\frac{1}{N}\right) \tag{1}$$

$$\sigma_y = \left(\frac{1}{\sqrt{4\pi}}\right)\left(\frac{1}{\sqrt{R}}\right)\left(\sqrt{\frac{P_b}{E_{cm}\mathcal{L}_g}}\right)\left(\sqrt{N}\right) \tag{2}$$

$$\Upsilon = \left(\frac{5\sqrt{\pi}r_e^2}{6\alpha mc^2}\right)\left(\frac{\sqrt{R}}{1+R}\right)\left(\sqrt{\frac{E_{cm}^3\mathcal{L}_g}{P_b}}\right)\left(\frac{\sqrt{N}}{\sigma_z}\right) \tag{3}$$

$$D_y = \left(16\pi mc^2 r_e\right)\left(\frac{R}{1+R}\right)\left(\frac{\mathcal{L}_g}{P_b}\right)(\sigma_z) \tag{4}$$

$$n_\gamma = 2.54U_0(\Upsilon)F\,, \quad \delta_E = 1.24\Upsilon U_1(\Upsilon)F \tag{5}$$

$$F = \left(\frac{5\sqrt{\pi}r_e^2}{3\lambda_c}\right)\left(\frac{\sqrt{R}}{1+R}\right)\left(\sqrt{\frac{E_{cm}\mathcal{L}_g}{P_b}}\right)\left(\sqrt{N}\right). \tag{6}$$

The advantage of organizing the independent and dependent parameters in such a way lies in its convenience for design optimization in the multidimensional parameter space, since in most situations many of the independent parameters can be fixed. For example, in this paper, we set $E_{cm} = 5$TeV

and $\mathcal{L}_g = 10^{35}\text{cm}^{-2}\text{s}^{-1}$ as our goal in energy and luminosity frontiers. For laser-driven acceleration, we assume $R = 1$ for reasons that will be explained later in this section. Furthermore, given maximum wall plug power, it is often adequate to consider P_b at a few discrete values corresponding to different accelerator efficiencies. Then for each fixed value of P_b we are left with only two independent parameters $\{N, \sigma_z\}$ to vary, and all the dependent parameters can thus be conveniently visualized in a surface or contour plot, as will be shown in the next section.

The design approach given here can be extended to integrate more collider parameters and the associated boundary conditions into the process of constrained optimization. For example, the beam size σ_y is related to two other important parameters: the normalized rms emittance ε_y and the betafunction at IP β_y by $\sigma_y = \sqrt{\beta_y \varepsilon_y / \gamma}$. Once σ_y is determined, ε_y and β_y can be chosen according to other constraints, and vice versa. One constraint that is of immediate importance for the IP is the Oide limit [7], which sets the minimum achievable beam size: $\sigma_{min}[\text{m}] = 1.7 \times 10^{-4} \varepsilon_y[\text{m}]^{5/7}$. Here we have used in the Oide limit a smaller numerical factor proposed by Irwin [8]. For later use, we define $F_{oide} = \sigma_y / \sigma_{min}$, the Oide limit is violated if $F_{oide} < 1$.

Before going to the exploration of parameter space using Eqs.(1-6), it is instructive to look at the more transparent scaling laws in two dimensional parameter space $\{N, \sigma_z\}$ when $\{E_{cm}, \mathcal{L}_g, P_b, R\}$ are considered fixed

$$f_c \sim 1/N \,, \quad \sigma_y \sim \sqrt{N} \,, \quad D_y \sim \sigma_z \,, \quad \Upsilon \sim \sqrt{N}/\sigma_z \tag{7}$$

$$n_\gamma \sim U_0(\Upsilon)\sqrt{N} \,, \quad \delta_E \sim \Upsilon U_1(\Upsilon)\sqrt{N}. \tag{8}$$

In the limit $\Upsilon \gg 1$, $U_0(\Upsilon) \to 1/\Upsilon^{1/3}, \Upsilon U_1(\Upsilon) \to 1/\Upsilon^{1/3}$. Eq.(8) becomes

$$n_\gamma \sim (N\sigma_z)^{1/3} \,, \quad \delta_E \sim (N\sigma_z)^{1/3}. \tag{9}$$

We see from Eqs.(7,9) that once in the high Υ regime there are two approaches to reduce the effects of beamstrahlung: either by reducing N or by reducing σ_z. The consequences on the collider design and the implied restrictions on the approaches, however, can be quite different. Reducing N requires f_c to be increased and σ_y decreased, thus the approach is limited by the constraints on f_c and σ_y. Reducing σ_z, on the other hand, is not directly restricted in this regard. Also the dependencies of Υ on the two approaches are quite the opposite. The second approach clearly demonstrates the case that beamstrahlung can indeed be suppressed by having larger Υ.

We now come to explain why it is reasonable to assume round beam $R = 1$. The current designs of linear colliders at 0.5 TeV are all based on damping ring technology which provides much smaller emittance in the vertical dimension. Taking advantage of this feature, beam distribution at the IP has been made

very flat, $R \gg 1$, to suppress beamstrahlung. However, first of all, it is not clear at this point what would be the injector of choice for future laser-driven accelerator, if emittances can be made as asymmetrical as in the damping ring, or if possible, would it be compatible with, for example, transverse focusing channel of the acceleration scheme. Secondly, as will be shown in the next section for round beam, the required beam size is already in the Å level. A flat beam requires the beam size in one dimension be made even smaller, thus pushing the limit for tight beam positioning control. Nonetheless, one should keep in mind that making $R \gg 1$ is still a knob for further suppression of beamstahlung, even in strong quantum regime as can be seen from Eqs.(1-6).

Parameter Optimization

Using the formulas provided in the previous section: Eqs.(1-6), we are now ready to explore the parameter space. As mentioned before we will consider the situation with $\{E_{cm} = 5\text{TeV}, \mathcal{L}_g = 10^{35}\text{cm}^{-2}\text{s}^{-1}, R = 1\}$. Assuming wall plug power for such a collider is limited to 2 GW [8], and the overall "wall plug to beam" efficiency is within the range of 0.1% to 10%, we will look at three cases with P_b being 2 MW, 20 MW and 200MW, respectively.

Figure 1 shows the contour plots of parametric scans for the cases with P_b = 2MW (left column) and 20MW (right column). Due to page limitation, we show only a few out of many quantities that can be monitored in $\{N(10^8), \sigma_z(\mu\text{m})\}$ space, they are, starting from the top row: n_γ, Υ and σ_y(nm). From these scans one may chose optimal operation point $\{N, \sigma_z\}$ based on various constraints imposed on the independent as well as dependent quantities. Using the plots in the bottom row one can also determine ε_y(nm) and $\beta_y(\mu\text{m})$ at different values of σ_y, and from there to check F_{oide}. The type of parametric scans shown here are used as a guide to pick specific parameter sets given in Table 1 for three values of beam power. Several performance parameters computed from the formulas are given in Table 2, some of them can be directly compared with simulations. It is noted here we have chosen to make n_γ significantly less than 1 and same for all three cases, and violate the Oide limit by about 10% on purpose to relax other parameters.

High Υ IP Simulation

Although the simple formula, Eq.(5), takes into account strong quantum beamstrahlung with high Υ, some important effects are nonetheless neglected, for example, disruption and multiphoton processes [6]. It is therefore necessary to examine its predictions with full-blown simulations. We use a Monte-Carlo simulation code recently developed by Yokoya [5] to study QED processes at the IP for e^+e^- and $\gamma\gamma$ colliders. This code is a superset of the well-known code ABEL by the same author. Care has been taken to ensure that there is

enough resolution in the simulation at such high Υ values to yield reliable QED prediction. This is established by verifying that results changes insignificantly by changes of resolution grids.

Figure 2 gives the differential e^+e^- luminosities for the case I, II, III in Table 1. It is noted that the luminosity spectrum is characterized by an outstanding core at the full energy and a very broad, nearly flat halo. One see from Table 3, taking case II for example, although on average the beam loses 26% of its energy and has a rms energy spread of 36%, the core itself within 1% of full energy still accounts for 65% of the geometrical luminosity. The outstanding core is more than two orders of magnitude above the halo. The sharpness and the high luminosity of the core is rather surprising but pleasantly so. Comparing simulation results in Table 3 for n_γ and δ_E with that calculated from the formulas in Table 2, one see the agreement varies from being reasonably good at lower Υ to rather poor at higher Υ. It seems to indicate that the formulas can be used only as a rough guideline for collider design at high Υ. It is interesting to note that the core luminosity is somewhat larger for the case with higher beamstrahlung loss, which is probably due to disruption enhancement as indicated by the larger value of D_y in Table 2.

Another major deteriorating process at high Υ is coherent pair creation. The number of pairs created per primary electron, n_p, is given in Table 2 by formulas [6] and in Table 3 by simulations. According to our simulations the incoherent pair creation is 2 to 3 orders of magnitude smaller than that of the coherent pairs, thus negligible. Finally we point out that such a differential luminosity spectrum should be rigorously assessed together with the background of beamstrahlung photons and coherent pairs from the point of view of particle physics and detector considerations. Only then, one may judge if operation of colliders at high Υ regime is indeed a viable approach for high energy physics applications.

ACCELERATOR CONSIDERATIONS

As seen from Eq.(9), an effective way to suppress beamstrahlung is to reduce σ_z, which naturally favors laser acceleration as it offers much shorter acceleration wavelength than that of conventional microwaves. For laser wakefield acceleration, typical wavelength of accelerating wakefield is ~ 100 μm, which is in the right range for the required bunch length in Table 1. Laser wakefield acceleration [9,10] has been an active area of research in recent years primarily due to the major technological advance in short pulse TW lasers [11]. The most recent experiment at RAL has demonstrated an acceleration gradient of 100 GV/m and produced beam-like properties with 10^7 accelerated electrons at 40MeV $\pm$ 10% and a normalized emittance of $\varepsilon < 5\pi$ mm-mrad [12].

For beam parameters similar to that in Table 1, we consider a laser wakefield accelerator system consisting of multiple stages with a gradient of 10 GeV/m.

With a plasma density of $10^{17}\mathrm{cm}^{-3}$, such a gradient can be produced in the linear regime with more or less existing T^3 laser, giving a plasma dephasing length of about 1 m [13]. If we assume a plasma channel tens of μm in width can be formed at a length equals to the dephasing length, we would have a 10 GeV acceleration module with an active length of 1 m. Of course, creating and maintaining a plasma channel of the required quality is no simple matter. To date, propagation in a plasma channel over a distance of up to 70 Rayleigh lengths (about 2.2 cm) of moderately intense pulse ($\sim 10^{15}\mathrm{W/cm}^2$) has been demonstrated [14]. New experiment aiming at propagating pulses with intensities on the order of $10^{18}\mathrm{W/cm}^2$ (required for a gradient of 10 GeV/m) is underway [13].

Table 1. Beam Parameters at Three Values of Beam Power

CASE	P_b(MW)	$N(10^8)$	f_c(kHz)	ε_y(nm)	$\beta_y(\mu\mathrm{m})$	σ_y(nm)	$\sigma_z(\mu\mathrm{m})$
I	2	0.5	50	2.2	22	0.1	0.32
II	20	1.6	156	25	62	0.56	1
III	200	6	416	310	188	3.5	2.8

Table 2. Results Given By the Formulas

CASE	Υ	D_y	F_{oide}	n_γ	δ_E	n_p	$\mathcal{L}_g(10^{35}\mathrm{cm}^{-2}\mathrm{s}^{-1})$
I	3485	0.93	0.89	0.72	0.2	0.19	1
II	631	0.29	0.89	0.72	0.2	0.12	1
III	138	0.081	0.91	0.72	0.2	0.072	1

Table 3. Results Given By CAIN Simulations

CASE	n_γ	δ_E	σ_e/E_0	n_p	$\mathcal{L}/\mathcal{L}_g(\mathrm{W_{cm}} \in 1\%)$	$\mathcal{L}/\mathcal{L}_g(\mathrm{W_{cm}} \in 10\%)$
I	1.9	0.38	0.42	0.28	0.83	1.1
II	0.97	0.26	0.36	0.12	0.65	0.80
III	0.84	0.21	0.32	0.06	0.62	0.75

Although a state-of-the-art T^3 laser, capable of generating sub-ps pulses with 10s of TW peak power and a few Js of energy per pulse [11], could almost serve the need for the required acceleration, the average power or the rep rate of a single unit is still quite low, and wall-plug efficiency inadequate. In addition, injection scheme and synchronization of laser and electron pulse from

stage-to-stage to good accuracy have to be worked out. Yet another important consideration is how to generate and maintain the small beam emittance in the transverse focusing channel provided by plasma wakefield throughout the accelerator leading to the final focus. There are various sources causing emittance growth, multiple scattering [15], plasma fluctuations [16] and mismatching between acceleration stages, to name just a few. Should the issues of guiding, staging, controllability, emittance preservation, etc. be worked out, there is hope that wakefields excited in plasmas will have the necessary characteristics for particle acceleration to ultrahigh energies.

CONCLUSIONS

We have explored the possibilities of operating a 5 TeV linear collider in the strong quantum beamstrahlung regime. To take the full advantage of quantum suppression of beamstrahlung, we have searched a large space of multidimensional collider parameters for the preferred regime of operation. By making collider scaling laws transparent, we found that reducing bunch length is an effective approach to suppress beamstrahlung, which naturally favors laser-driven acceleration. The prediction of scaling laws has been checked with full-blown IP simulations, and the results are quite encouraging. We have discussed the implied requirements for laser wakefield acceleration. The parameters of a 10 GeV module in a 5 TeV collider vision demonstrates both encouraging and sobering features that calls for further developments and innovations.

REFERENCES

1. Himel T., Siegrist J., AIP Conf. Proc., **130**, 602 (1985).
2. Chen P., Yokoya K., *Phys. Rev. Lett.*, **61**, 1101 (1988).
3. Blankenbecler R., Drell S., *Phys. Rev. D*, **37**, 3308 (1988).
4. Jacob M., Wu T. T., *Nucl. Phys.*, **B318**, 53 (1989).
5. For code and manual, see http://jlcux1.kek.jp/subg/ir/Program-e.html.
6. Yokoya K., Chen P., *Frontiers of Particle Beams*, **400**, 415 (1992).
7. Oide K., *Phys. Rev. Lett.*, **61**, 1713 (1988).
8. Irwin J., AIP Conf. Proc., **335**, 3 (1995).
9. Tajima T., Dawson J., *Phys. Rev. Lett.*, **43**, 267 (1979).
10. For recent experiment see Nakajima K., et. al., these proceedings.
11. For a review, see Downer M. C., Siders C. W., these proceedings.
12. For reference see Chattopadhyay S., et. al., Snowmass'96, LBL-39655, (1996).
13. Leemans W. P., et.al., *IEEE Trans. on Plasma Science*, **24**, 331 (1996).
14. Durfee III C. G., Milchberg H. M., *Phys Rev. Lett.* **71**, 2409 (1993).
15. Montague B. W., Schnell W., AIP Conf. Proc., **130**, 146 (1985).
16. Horton W., Tajima T., et.al., *Phys. Rev. A*, **31**, 3937 (1985).

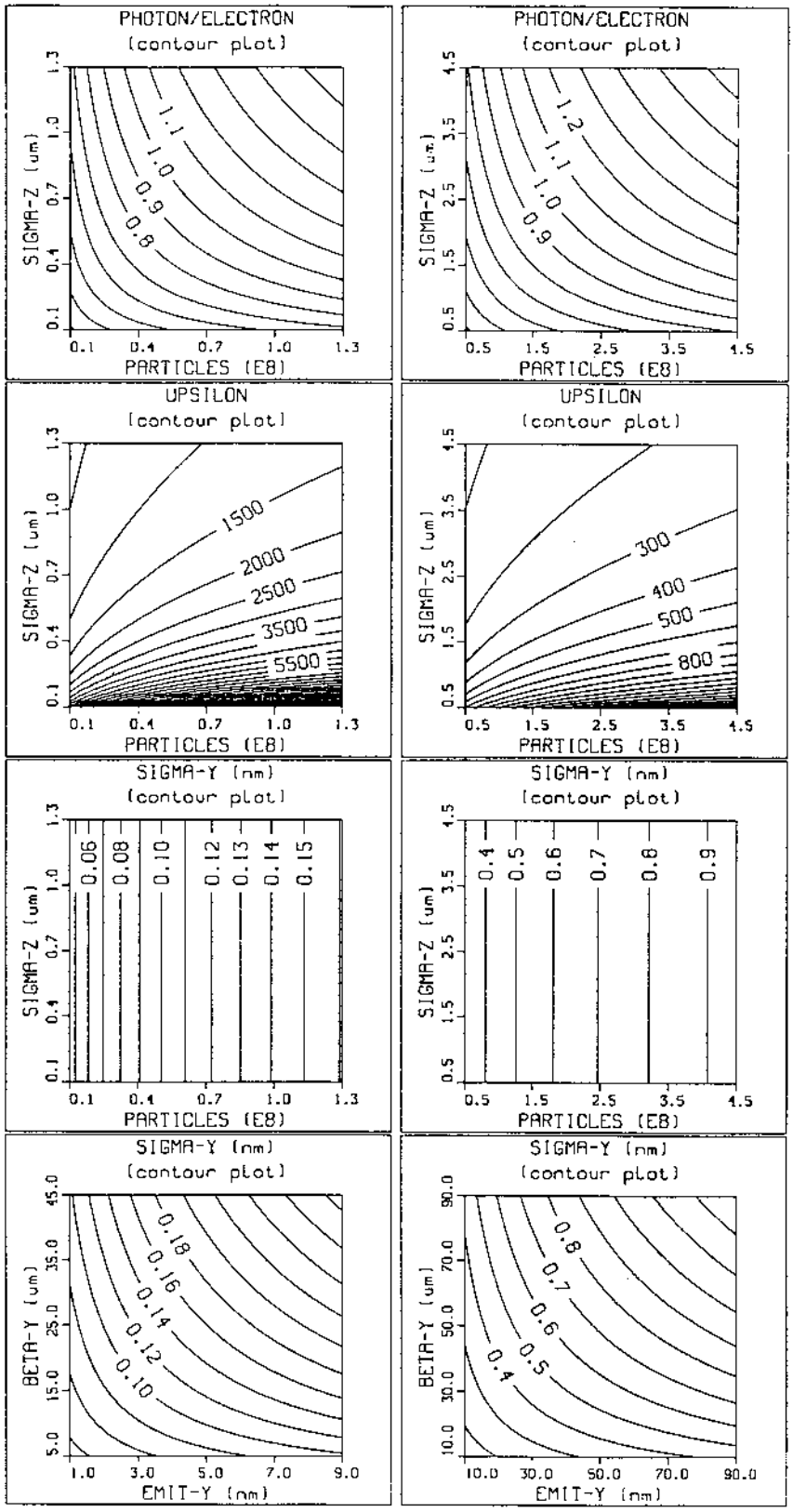

FIGURE 1. Parameter scans for P_b = 2MW (column 1) and 20MW (column 2).

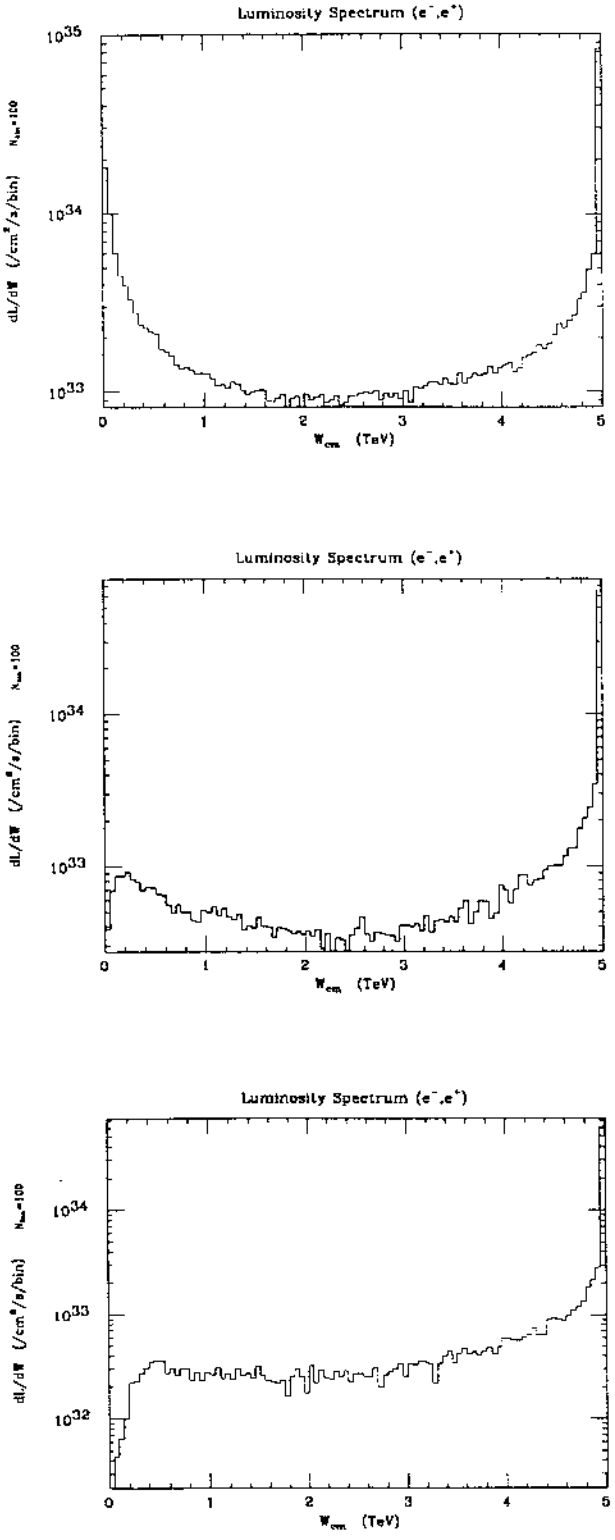

FIGURE 2. e^+e^- luminosity spectrum for case I (top), II (middle), III (bottom).